

SUPPLEMENTARY DATA

A serendipitous phosphonocarboxylate complex of boron: when vessel becomes reagent

Katarzyna M. Błażewska,^{a,b} Ralf Haiges,^a Boris A. Kashemirov,^a Frank H. Ebetino,^c Charles E. McKenna^{*a}

^a Department of Chemistry, University of Southern California, Los Angeles, CA 90089-0744, USA; Fax: +1 310 740 0930; Tel: +1 310 740 2698; E-mail: mckenna@usc.edu

^b Institute of Organic Chemistry, Technical University of Łódź, Zeromskiego St. 116, 90-924 Łódź, Poland; Fax: +48 42 636 55 30; Tel: +48 42 631 31 46

^c Warner Chilcott Pharmaceuticals, Mason, OH 45040, USA; Tel: +1 513 622 3630

Table of Contents	S:
General methods, reagents and materials.....	3
HPLC and NMR detection of 5 and 6	3
pH and temperature effects (3)	3
Vessel effects (3)	4
pH and temperature effects (1)	4
Vessel effects (1)	4
HRMS studies	4
Detection of 11B NMR signal	4
Crystallization of 5 compound isolated from evaporate of 3 and X-ray crystallographic analysis.....	4
Identification of the source of boron	5
3 boron complex generation from borate.....	5
Figure S1. HPLC trace of the “ghost” compound from 3-E1 after isolation by preparative HPLC.....	5
Figure S2. Same solution as in Figure S3, after being stored at rt, pH 7.4, for 27 h, 44 h, 72 h.	5
Figure S3. HPLC trace of 3 enantiomers (E1, E2) from 3 racemate sample.	6
Figure S4. ¹ H NMR (D ₂ O, pH 3.6, 400 MHz) of the “ghost” compound from 3-E1 after preparative HPLC isolation as above.....	6
Figure S5. ¹ H NMR of product from reaction of 3 with aq. sodium borate (rt). Compare with Figure S4.	7
Figure S6. ³¹ P NMR of product from reaction of 3 with aq. sodium borate (rt). Compare with Figure 3 in the manuscript.....	7
Figure S7. FAB HRMS of the isolated “ghost” compound derived from 3-E2.	8
Figure S8. ORTEP drawings of both (S,S)-3 and (R,R)-3 dimer boron complexes formed in the crystal.....	9
Figure S9. Structures of diastereomeric dimer boron complexes.	9
Figure S10. Unit cell of the (R,R)-3 and (S,S)-3 dimer boron complex.....	10
Table S1. Crystal data and structure refinement for C ₂₀ H ₁₄ BN ₄ O ₁₆ P ₂	11
Table S2. Atomic coordinates (× 10 ⁴) and equivalent isotropic displacement parameters (Å ² × 10 ³) for C ₂₀ H ₁₄ BN ₄ O ₁₆ P ₂	12
Table S3. Bond lengths [Å] and angles [°] for C ₂₀ H ₁₄ BN ₄ O ₁₆ P ₂	13
Table S4. Anisotropic displacement parameters (Å ² × 10 ³) for C ₂₀ H ₁₄ BN ₄ O ₁₆ P ₂	14

Table S5. Hydrogen coordinates ($\times 10^4$) and isotropic displacement parameters ($\text{\AA}^2 \times 10^3$) for C ₂₀ H ₁₄ BN ₄ O ₁₆ P ₂	15
Parameters and numerical results for Spartan calculations of dimer complexes of boron.....	16
Reference List.....	19

General methods, reagents and materials

Compound **1** was a gift from Procter & Gamble Pharmaceuticals, Inc. Compound **3** was synthesized by our published method.¹ All solvents and reagents were reagent grade, purchased commercially from Sigma-Aldrich, Inc. and used without further purification except as mentioned below. Triethylamine was freshly distilled before use. HPLC was carried out using a Dynamax Rainin Model SD – 200 pump equipped with a Shimadzu SPD – 10A VP UV Vis detector on ProntoSIL AX QN 8 × 150 mm and ProntoSIL AX QD 4 × 150 mm chiral columns (Bischoff Chromatography, Leonberg, Germany). The columns were eluted isocratically with 0.7 M TEAA in 75% MeOH at pH 5.8 for enantioseparation of **3**, or with 0.25 M TEAA in 75% MeOH at pH 6.9 for enantioseparation of **1**. NMR spectra were measured on Varian Mercury 400 and Bruker 250 spectrometers. Chemical shifts (δ) are reported in parts per million (ppm) relative to internal residual HDO in D₂O (pH ~12, δ 4.7) (¹H) or ext. H₃PO₄ (³¹P). Standard MS was performed using a Thermo-Finnigan LCQ DECA XP_{max} Ion Trap LC/MS/MS equipped with an ESI probe. HRMS analysis was performed at the UC Riverside MS Facility, using a VG-ZAB MS spectrometer operated in FAB mode. Mass spectra simulations were calculated using the iMass program for Apple Mac computers. UV spectra were acquired on a Beckmann Coulter DU 800 spectrophotometer. Concentrations of **3** and **5** in aqueous solution (pH 6.3) were assigned from their UV spectra, using $\epsilon = 6450$ at 280 nm, as determined for **3**.¹

Geometric direct minimization calculations were performed using the SPARTAN '08 Quantum Mechanics software suite: Release 132v4, using the RHF-SCF method and the 3-21G* basis set.

HPLC and NMR detection of **5** and **6**

In chiral HPLC separations of the **3** enantiomers, fractions were collected into “fresh” borosilicate glass test tubes (VWR, Inc.). Reanalysis of the isolated enantiomer fraction (~1-2 mg) after concentration by evaporation often revealed the presence of a small, early-eluting extra peak (Figure 2 in the manuscript). Due to its ephemeral nature (it decreased on standing or disappeared on heating in aq. solution at pH \geq 7), it was initially referred to informally as a “ghost” compound. The unprocessed **3** racemate did not give a detectable “ghost” peak on HPLC analysis (*cf.* Figure 2 in the manuscript). A similar phenomenon was observed with **1** enantiomer separations (data not shown), and it was found that enrichment in the “ghost” products **6** could be achieved by keeping sample size small (Figure 2/inset in the manuscript).

The “ghost” species from **3** (E1 enantiomer) could be isolated by preparative HPLC, giving a compound which when dissolved in 0.7 M TEAA in 75% MeOH at pH 5.8, 22 °C gave a single HPLC peak, ret. time 9.15 min at 1 mL/min elution from the AX QD column (Figure S1). After standing for 72 h at ~22 °C, at pH 7.4, re-analysis on the AX QD column showed disappearance of this peak, with one new peak created with ret. time 12.8 min, identified as **3**-E1 (Figure S2). An HPLC analysis of racemic **3** is presented in Figure S3.

The “ghost” compound **5** derived from **3**-E1 (or from **3**-E2) has distinct ¹H (Figure S4) and ³¹P (Figure 3 in the manuscript) NMR spectra, the latter showing a single peak at δ 11.9 in D₂O at pH 3.6, upfield from **3** itself ($\delta \geq$ 13). ³¹P NMR values for **3** were δ 12.9-13.0 (pH 2.8) to δ 15.6 (pH 7); for the **3** “ghost” (major) δ 11.8 – 11.9 (pH 2.8-7). This permitted convenient exploration of conditions that might affect the formation and stability of the “ghost” compounds derived from **3**.

The following experiments were carried out on 0.5 – 1 mg samples of **3** on preparative HPLC isolates of the **3** enantiomers after collection into “fresh” borosilicate glass test tubes, evaporation and storage in “fresh” borosilicate glass vials, unless otherwise noted.

The ³¹P NMR singlet of **6** at δ 12.2 ppm (pH 4.8), was accompanied by two other small singlets at δ ppm, both with approximately the same integration. These were not investigated, but might correspond to an asymmetric dimer.

pH and temperature effects (**3**)

- 3**-E1, 18 mM (UV) in H₂O, pH 6.2, heated to 90 °C, cooled to rt, sealed in a fresh glass ampule and kept at 5 – 7 °C for 1 yr: **3**, 90%; “ghost”, 10% (HPLC).
- As in a. but, after 4 mos: **3**, 96%, “ghost”, 4%.
- As in a. but, pH 7.5, after 3 mos: **3**, 100%.
- As in a. but, pH 7.0, after 13.5 mos: **3**, 100%.
- As in a. but, pH 4.8, after 4 d: **3**, 70%, “ghost”, 30%.
- As in a. but, 3 – 6 mM evaporated at pH 2.8 (H⁺ Dowex); then pH adjusted to 7: initially, **3** 60%, “ghost”, 40%; immediately after pH 7, **3** 59%, “ghost” 36%; new peak at δ 11.5 (5%).
- As in a. but, adjust pH to 6.5, 85 °C, 2 h or 4 d, rt; or 1 d, 5 °C: **3**, 100%.

It was concluded that acidic pH during evaporation favored “ghost” product formation, whereas near neutral

pH, it was converted back to **3**; this process was accelerated by heating in water. Similar results were obtained with solutions containing 5 mM MgCl₂ (data not shown).

Vessel effects (3)

- Vials rinsed with EtOH and then with H₂O and dried gave somewhat reduced yields of the **5** product at pH 2.8.
- When polypropylene vials were substituted for the glass vials, no **5** product formation could be detected under any of the above conditions.

pH and temperature effects (1)

- 1**, 30 mM, pH 4: **1**, 87% (δ 15.0), “ghost” product, 9% (δ 12.1); 47%-49% after 20 h, 5 °C or 42%-55% after 7 d rt.
- 1**, ~33 mM, pH 2.5, 20 h: precipitate.
- 1**, 33 mM, pH 4.6, rt or after 20 h (5 °C): 95% **1**, ~4-5% “ghost” product.
- At pH \geq 7.4 and 5 °C, no “ghost” product was detected after up to 15 d storage.

Vessel effects (1)

- 1**, 11-16 mM aq. solutions, pH 4.6 – 5.3 after evaporation in repeatedly washed (dil. HCl) borosilicate glassware and storage in polypropylene vials, or in a teflon bottle gave directly after evaporation, or after 2, 5, or 7 d storage, 100% **1** by ³¹P NMR (no detectable “ghost” product).

It was concluded that the same pattern as with **3** was observed; however at low pH **1** gives a precipitate whose composition was not determined.

HRMS studies

The purified **5** isolate from **3**-E2 was subjected to high resolution mass spectrometric analysis using a FAB instrument. The dominant peak was observed at 579.0488 M/Z, an excellent fit for ¹²C₂₀¹H₁₈¹⁶O₁₂¹⁴N₄³¹P₂¹¹B: [M – H][–] calcd, 579.049 but was a poor fit to a carbon-centered complex ([M – H][–] calcd, 579.0318). The predicted [M – H – 1][–] peak at ~20% of the [M – H][–] peak intensity, due to a naturally abundant ¹⁰B ion, is also observed (Figure S5).

Detection of ¹¹B NMR signal

A comparable sample was found to have a broad resonance at ~7-8 ppm (160.42 MHz quartz sample tube; relative to ext. 15% BF₃ • OEt₂ in CDCl₃).

Crystallization of **5** compound isolated from evaporate of **3** and X-ray crystallographic analysis

Racemic **3** (2 mg) was placed in a fresh borosilicate vial (4 mL) and dissolved in 250 μ L H₂O (heating applied to complete dissolution); 9 μ L TFA was added. The mixture was brought to rt and the solution evaporated in the air for 10 d to give a solid crystalline residue.

The single crystal X-ray diffraction data was collected on a Bruker 3-circle platform diffractometer equipped with a SMART CCD (APEX) detector with the χ -axis fixed at 54.74° and using Mo K α radiation (Graphite monochromator) from a fine-focus tube. The diffractometer was equipped with a Cryo Industries Cryocool-LN2 apparatus for low-temperature data collection, using controlled liquid nitrogen boil-off. The crystals were mounted on a goniometer head using a CryoLoop and PFPE oil. Cell constants were determined from 60 ten-second frames. A complete hemisphere of data was scanned on omega (0.3°) with a run time of ten seconds per frame at a detector resolution of 512 \times 512 pixels using the SMART software package.² A total of 1,271 frames were collected in three sets and a final set of 50 frames, identical to the first 50 frames, was also collected to determine any crystal decay. The frames were then processed on a PC, running Windows 2000 software, by using the SAINT software package³ to give the hkl files corrected for Lp/decay. The absorption correction was performed using the SADABS program.⁴ The structure was solved by the direct method using the SHELX-90 program and refined by the least squares method on F^2 , SHELXL-97 incorporated in SHELXTL Suite 6.12 for Windows NT/2000.⁵ All non-hydrogen atoms were refined anisotropically. For the anisotropic displacement parameters, the U_{eq} is defined as one third of the trace of the orthogonalized U_{ij} tensor. ORTEP drawings were prepared using the ORTEP-3 for Windows V2.02 program.⁶ Further details of the crystal structure investigations reported in this paper may be obtained from the Cambridge Crystallographic Data Centre (CCDC), 12 Union Road, Cambridge CB2 1EZ (UK) (fax: +44 (1223)336-033 or email: deposit@ccdc.cam.ac.uk) by quoting the depositary number CCDC 794952.

The crystal structure analysis revealed a mixture of (*R,R*) and (*S,S*) **3** dimer boron complexes (Figure S8-S9)

formed for the crystal.

Identification of the source of boron

It was confirmed that the **5** compound was not formed from **3** under any of the following conditions: 1) exposure to the HPLC column without isolated sample evaporation; 2) prolonged exposure to TEAA buffer at pH 4-6 in repeatedly washed (dil. HCl) borosilicate glassware; 3) evaporation in repeatedly washed (dil. HCl) borosilicate glassware; 4) collection of HPLC fractions into polypropylene test tubes and evaporation in repeatedly washed (dil. HCl) borosilicate glassware. However, when HPLC fractions of **3** were collected into “fresh” VWR borosilicate glassware test tubes, a “ghost” peak was reproducibly detected.

3 boron complex generation from borate

3 (2.2 mg, 0.0077 mmol) was suspended in 0.5 mL H₂O and heated to dissolve (pH 2.7). To the resulting solution was added 0.7 M H₃BO₃ aq. (0.5 equiv, no change in pH). After evaporation to dryness at 100 °C (oil bath 4 h) a white solid was obtained that was suspended in small amount of D₂O, and dissolved by addition of 2.25 M aq. NaOH (final pH 5.7). The conversion of **3** into the product was 89% by ³¹P NMR.

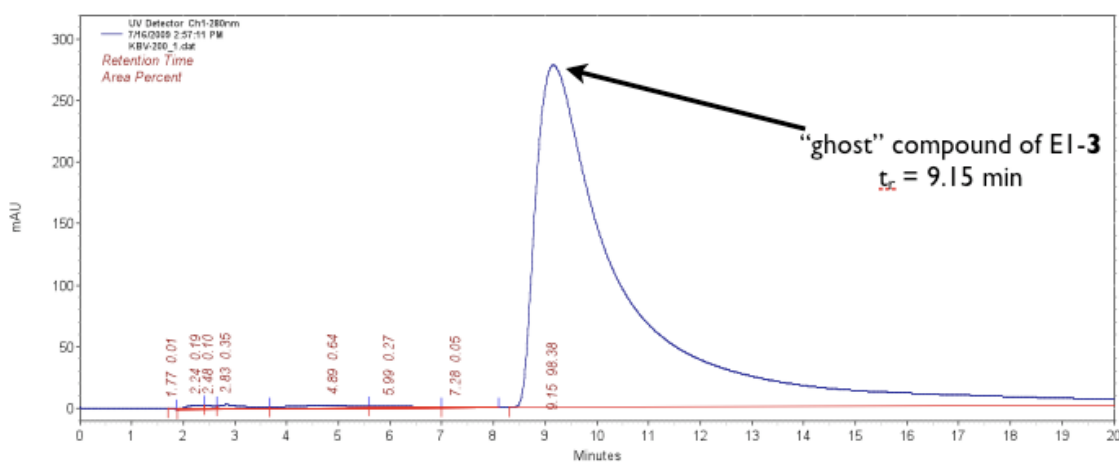


Figure S1. HPLC trace of the “ghost” compound from **3**-E1 after isolation by preparative HPLC. Conditions: AX QD 0.7 M TEA/AcOH in 75% MeOH, pH 5.8, flow rate 1 mL/min.

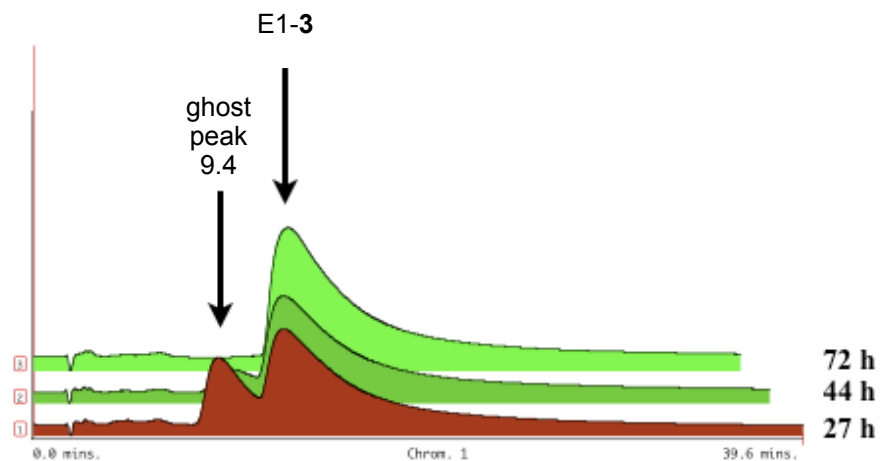


Figure S2. Same solution as in Figure S3, after being stored at rt, pH 7.4, for 27 h, 44 h, 72 h. Conditions: AX QD 0.7 M TEA/AcOH in 75% MeOH, pH 5.8, flow rate 1 mL/min.

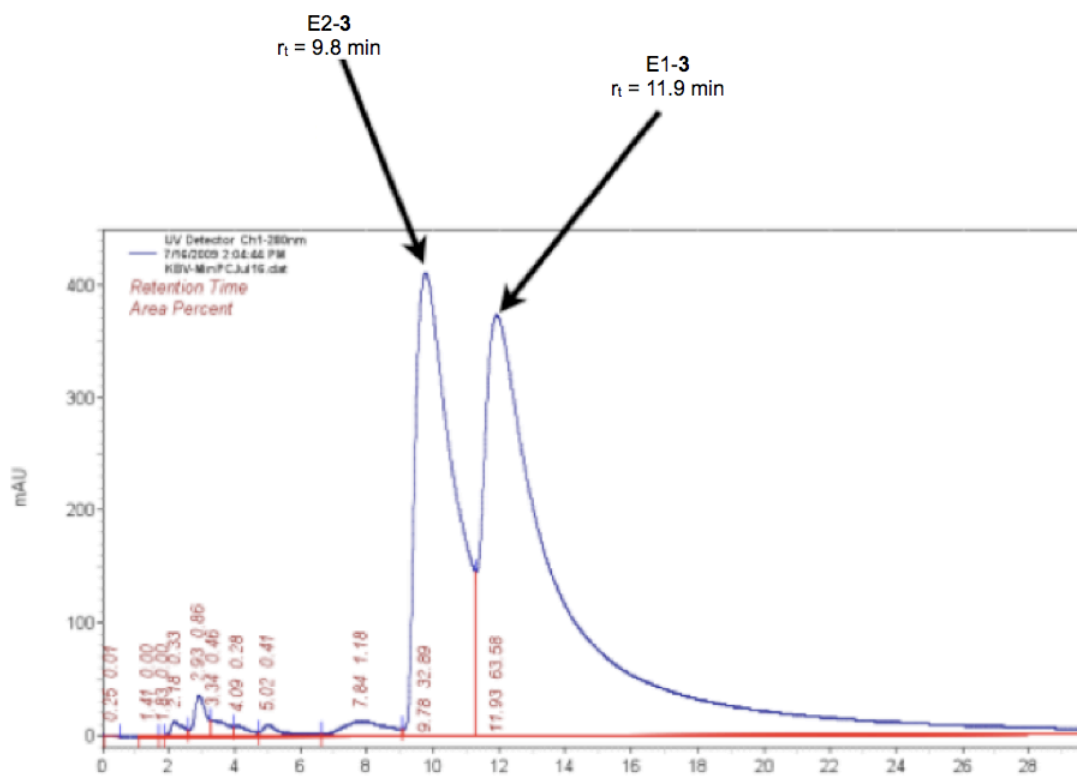


Figure S3. HPLC trace of **3** enantiomers (E1, E2) from **3** racemate sample.
HPLC conditions: as above, AX QD column, flow rate = 1 mL/min.

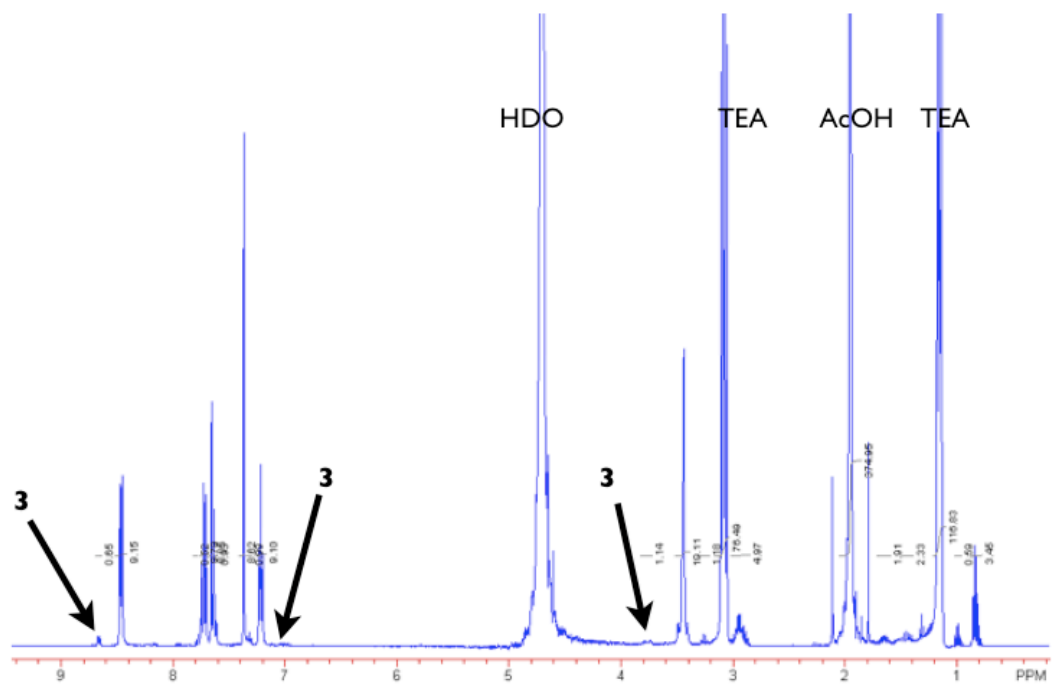


Figure S4. ¹H NMR (D₂O, pH 3.6, 400 MHz) of the “ghost” compound from **3**-E1 after preparative HPLC isolation as above.

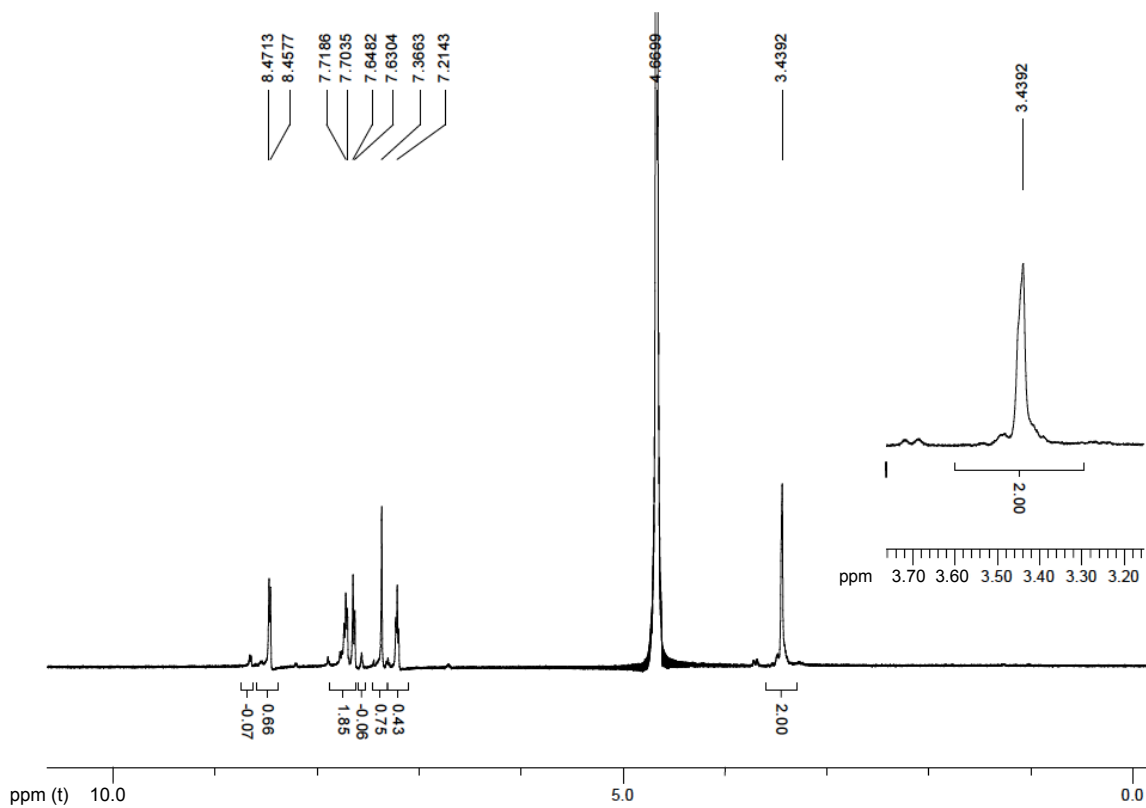


Figure S5. ^1H NMR of product from reaction of **3** with aq. sodium borate (rt). Compare with Figure S4.

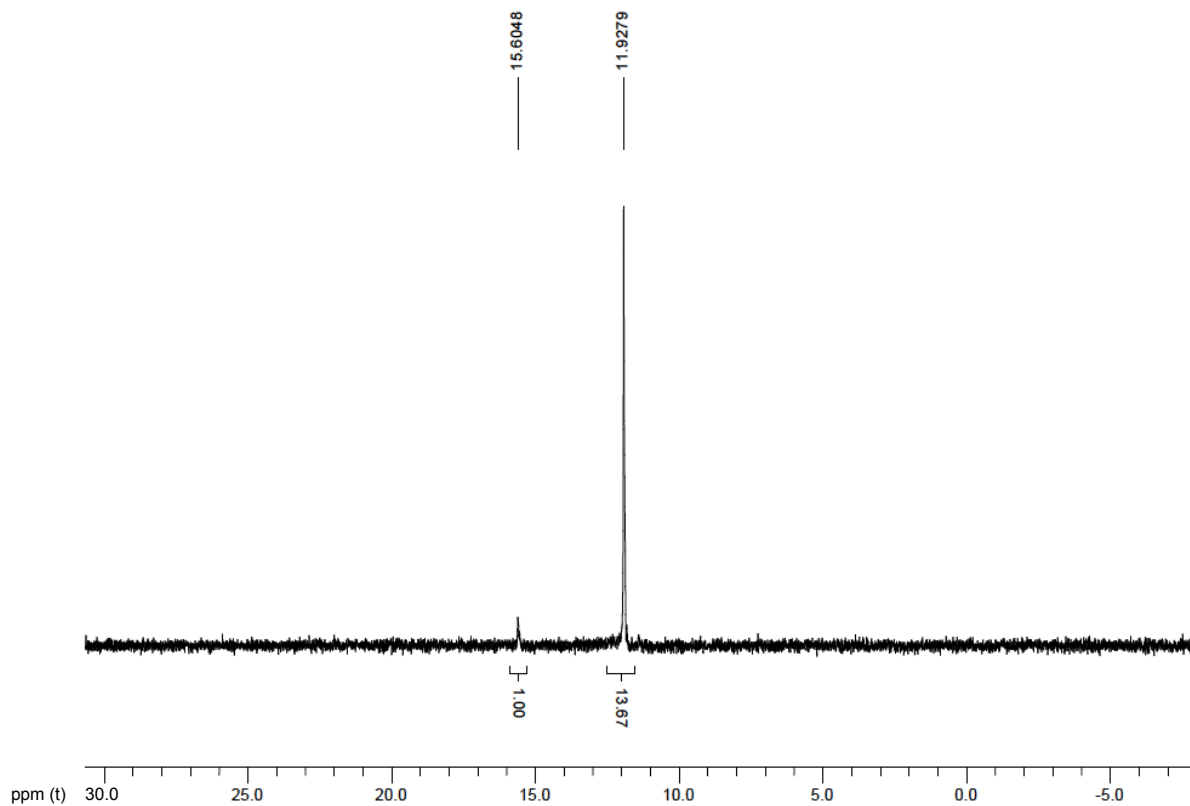


Figure S6. ^{31}P NMR of product from reaction of **3** with aq. sodium borate (rt). Compare with Figure 3 in the manuscript.

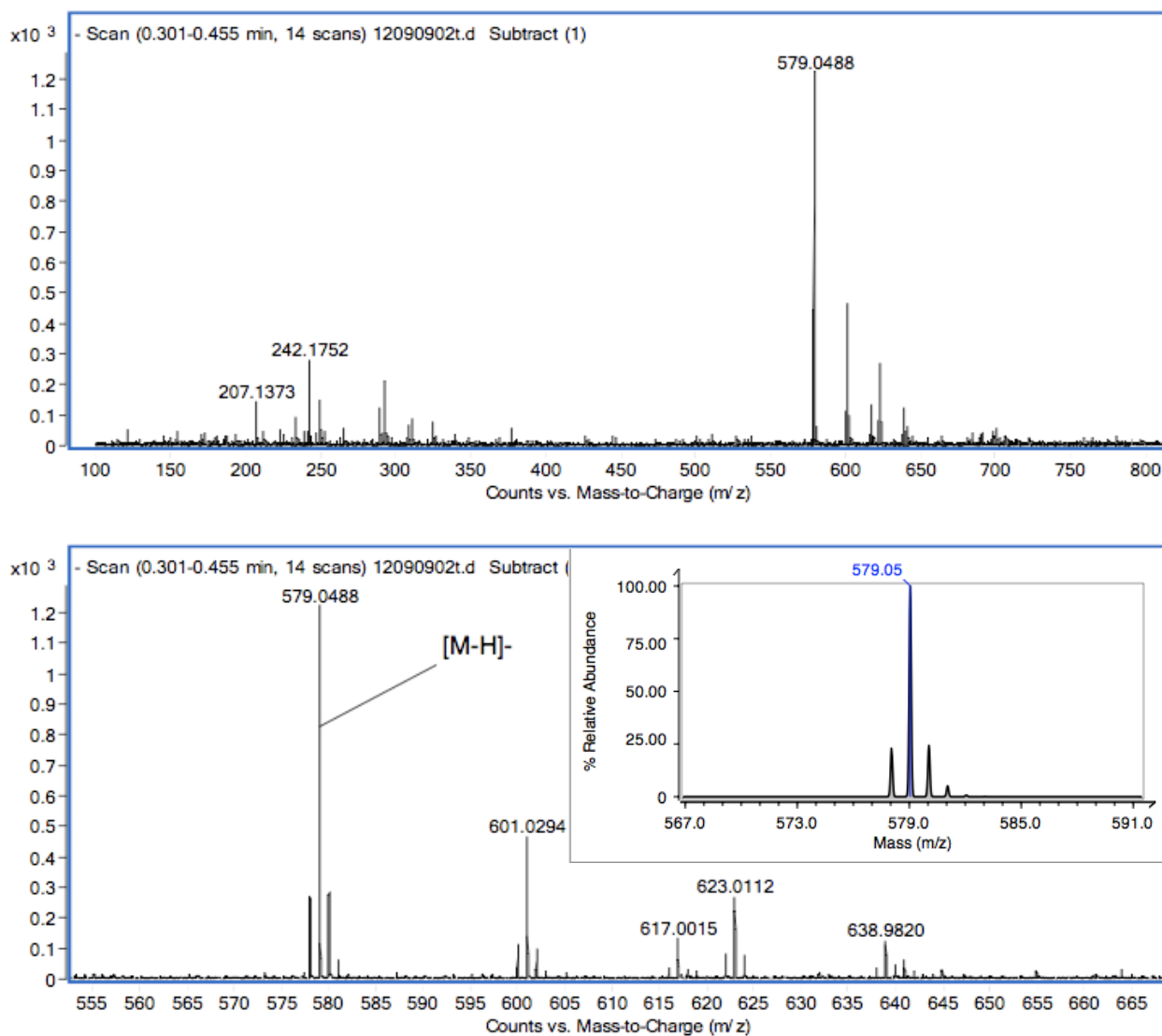


Figure S7. FAB HRMS of the isolated “ghost” compound derived from **3-E2**.
(Lower spectrum is an enlargement of the upper spectrum; inset, predicted isotopic distribution pattern for $C_{20}H_{18}O_{12}N_4P_2B$ near M/Z 579 predicting a 20% relative abundance $[M - H - 1]^-$ peak for a ^{10}B ion.

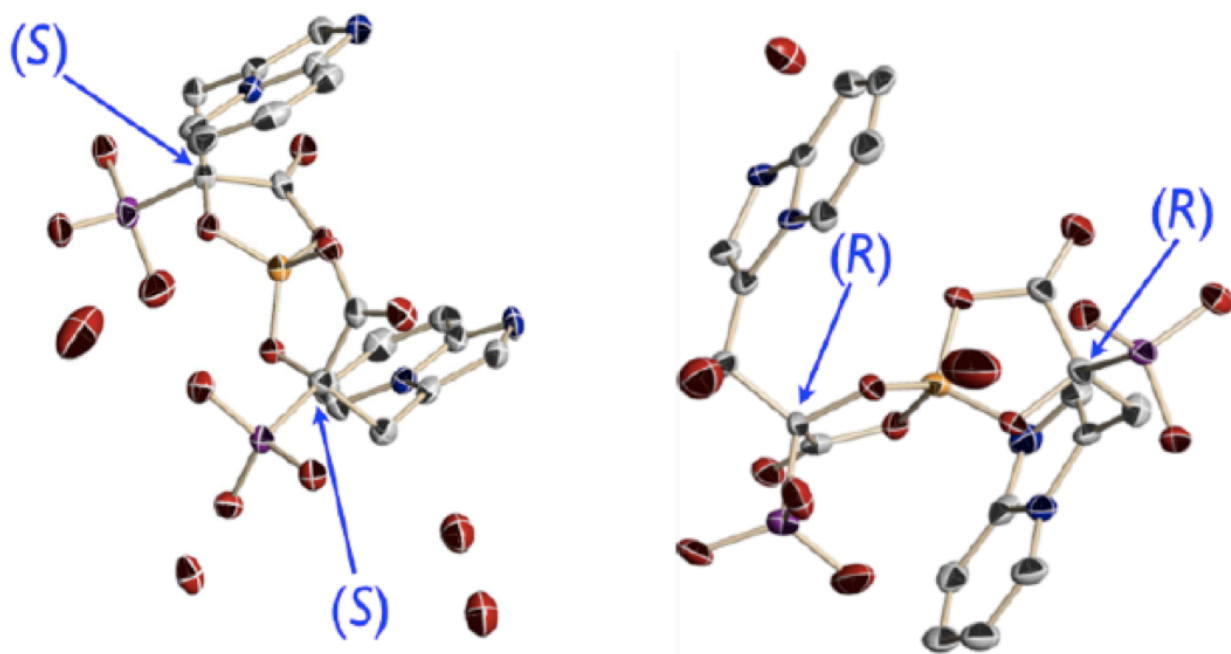


Figure S8. ORTEP drawings of both (*S,S*)-**3** and (*R,R*)-**3** dimer boron complexes formed in the crystal. Thermal ellipsoids are shown at the 50% probability level.

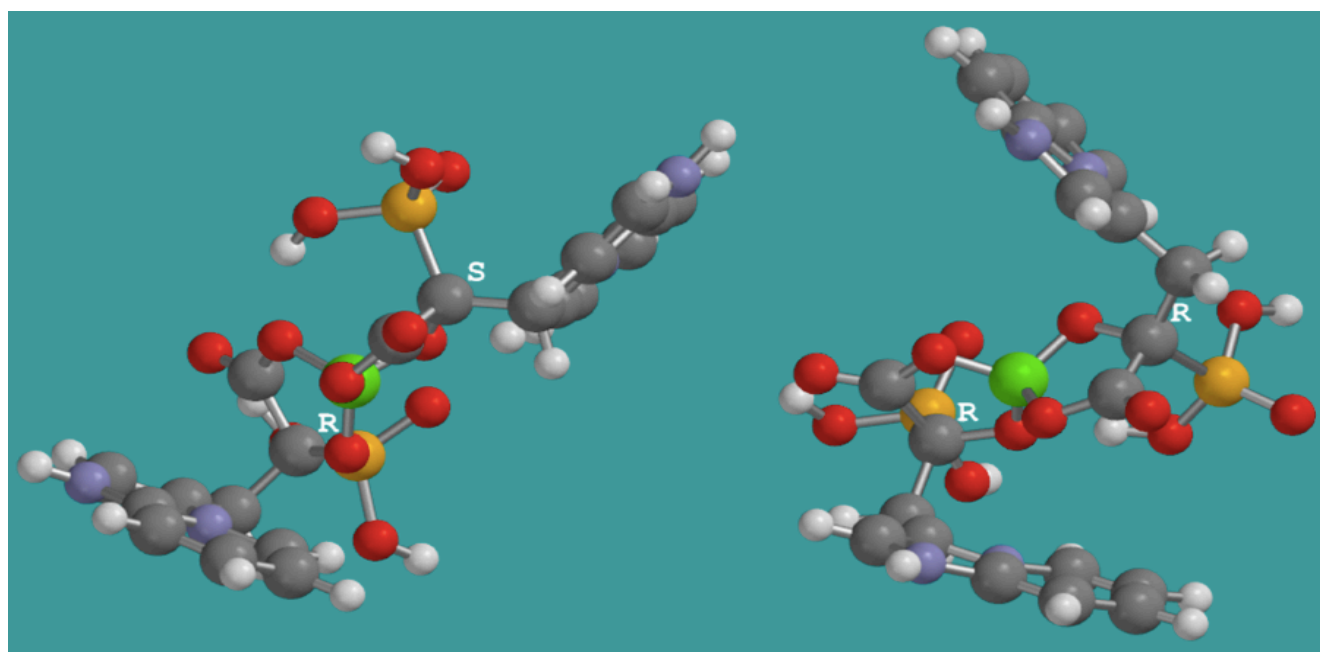


Figure S9. Structures of diastereomeric dimer boron complexes. The structure calculated by geometric direct minimization using the Spartan '08 Quantum Mechanics software suite. Left: heterochiral, (*R,S*) dimer complex. Right: homochiral, (*R,R*) dimer complex (*cf.* Figure S8, S10). Thermal ellipsoids are shown at the 50% probability level.

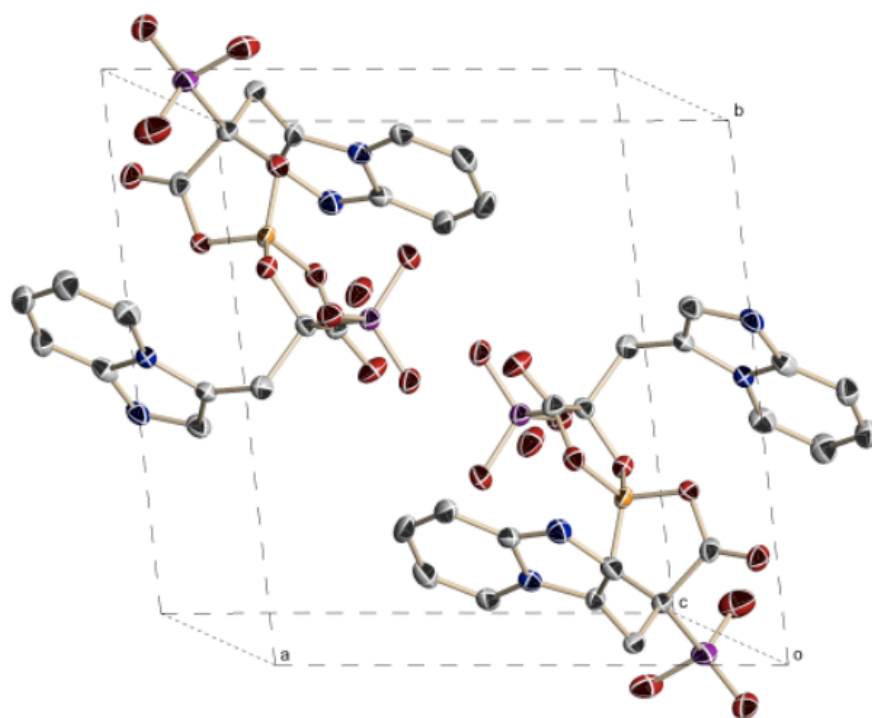


Figure S10. Unit cell of the (*R,R*)-**3** and (*S,S*)-**3** dimer boron complex. Thermal ellipsoids are shown at the 50% probability level.

Table S1. Crystal data and structure refinement for C₂₀H₁₄BN₄O₁₆P₂.

Identification code	kv89_0m	
Empirical formula	C ₂₀ H ₂₀ BN ₄ O ₁₃ P ₂	
Formula weight	597.15	
Temperature	143(2) K	
Wavelength	0.71073 Å	
Crystal system	Triclinic	
Space group	P-1	
Unit cell dimensions	a = 10.3622(7) Å	α = 73.036(3)°
	b = 11.2452(8) Å	β = 79.538(3)°
	c = 11.8058(9) Å	γ = 84.082(3)°
Volume	1292.10(16) Å ³	
Z	2	
Density (calculated)	1.535 Mg/m ³	
Absorption coefficient	0.243 mm ⁻¹	
F(000)	614	
Crystal size	0.15 x 0.12 x 0.10 mm ³	
Theta range for data collection	1.83 to 27.48°	
Index ranges	-12 ≤ h ≤ 13, -13 ≤ k ≤ 14, 0 ≤ l ≤ 15	
Reflections collected	5588	
Independent reflections	5588 [R(int) = 0.0398]	
Completeness to theta = 27.48°	94.1%	
Absorption correction	Multi-scan	
Transmission factors	min/max: 0.794	
Refinement method	Full-matrix least-squares on F ²	
Data / restraints / parameters	5588 / 0 / 377	
Goodness-of-fit on F ²	1.013	
Final R indices [I > 2σ(I)]	R1 = 0.0777, wR2 = 0.2124	
R indices (all data)	R1 = 0.1142, wR2 = 0.2362	
Largest diff. peak and hole	0.681 and -0.913 e.Å ⁻³	

Table S2. Atomic coordinates ($\times 10^4$) and equivalent isotropic displacement parameters ($\text{\AA}^2 \times 10^3$) for $\text{C}_{20}\text{H}_{14}\text{BN}_4\text{O}_{16}\text{P}_2$.

U(eq) is defined as one third of the trace of the orthogonalized Uij tensor.

	x	y	z	U(eq)
B(1)	8703(4)	7631(4)	2658(4)	20(1)
C(1)	10091(4)	8509(4)	3518(4)	24(1)
C(2)	9180(4)	9536(4)	2880(4)	20(1)
C(3)	8360(4)	10190(4)	3797(4)	24(1)
C(4)	7500(4)	9295(4)	4733(4)	23(1)
C(5)	7652(4)	8627(4)	5876(4)	24(1)
C(6)	5767(4)	8084(4)	5574(4)	24(1)
C(7)	4577(4)	7594(4)	5624(5)	30(1)
C(8)	3945(4)	8008(4)	4666(5)	36(1)
C(9)	4468(4)	8948(4)	3635(5)	33(1)
C(10)	5644(4)	9406(4)	3606(4)	27(1)
C(11)	7440(4)	5909(4)	3053(4)	25(1)
C(12)	8296(4)	6064(4)	1826(4)	21(1)
C(13)	9275(4)	4929(4)	1847(4)	26(1)
C(14)	10193(4)	4763(4)	2716(4)	23(1)
C(15)	10167(4)	4029(4)	3851(4)	27(1)
C(16)	11955(4)	5096(4)	3464(4)	26(1)
C(17)	13112(4)	5604(4)	3487(4)	29(1)
C(18)	13605(4)	6482(4)	2475(5)	35(1)
C(19)	12959(4)	6841(4)	1469(4)	35(1)
C(20)	11830(4)	6322(4)	1464(4)	29(1)
N(1)	6298(3)	8970(3)	4566(3)	22(1)
N(2)	6588(3)	7891(3)	6363(3)	27(1)
N(3)	11337(3)	5423(3)	2476(3)	23(1)
N(4)	11229(3)	4220(3)	4303(3)	27(1)
O(1)	8357(3)	8944(3)	2402(3)	24(1)
O(2)	9847(3)	7437(2)	3330(3)	21(1)
O(3)	10890(3)	8605(3)	4094(3)	29(1)
O(4)	11050(4)	9746(4)	940(4)	48(1)
O(5)	10773(3)	11525(3)	1982(3)	32(1)
O(6)	9149(3)	11278(3)	753(3)	35(1)
O(7)	8975(3)	7159(2)	1611(2)	21(1)
O(8)	7645(3)	6835(3)	3480(3)	23(1)
O(9)	6718(3)	5082(3)	3573(3)	32(1)
O(10)	8306(3)	6486(3)	-553(3)	29(1)
O(11)	6608(3)	5144(3)	804(3)	27(1)
O(12)	6386(3)	7445(3)	650(3)	28(1)
O(13)	5785(4)	6047(3)	8437(3)	38(1)
P(1)	10167(1)	10600(1)	1584(1)	28(1)
P(2)	7290(1)	6297(1)	632(1)	22(1)
O(23)	6675(5)	9687(4)	5072(7)	103(2)
P(1)	10164(1)	10598(1)	6582(1)	27(1)
P(2)	7290(1)	6299(1)	5631(1)	21(1)

Table S3. Bond lengths [Å] and angles [°] for C₂₀H₁₄BN₄O₁₆P₂.

B(1)-O(1)	1.438(5)	O(5)-P(1)	1.492(4)	C(11)-C(12)-P(2)	111.5(3)
B(1)-O(7)	1.454(6)	O(6)-P(1)	1.559(3)	C(13)-C(12)-P(2)	110.6(3)
B(1)-O(8)	1.502(5)	O(10)-P(2)	1.565(3)	C(14)-C(13)-C(12)	113.0(4)
B(1)-O(2)	1.507(5)	O(11)-P(2)	1.485(3)	C(15)-C(14)-N(3)	104.7(4)
C(1)-O(3)	1.195(5)	O(12)-P(2)	1.518(3)	C(15)-C(14)-C(13)	131.6(4)
C(1)-O(2)	1.343(5)	O(1)-B(1)-O(7)	114.6(3)	N(3)-C(14)-C(13)	123.8(4)
C(1)-C(2)	1.522(5)	O(1)-B(1)-O(8)	113.5(3)	C(14)-C(15)-N(4)	110.1(4)
C(2)-O(1)	1.414(5)	O(7)-B(1)-O(8)	104.1(3)	N(4)-C(16)-N(3)	106.1(4)
C(2)-C(3)	1.561(6)	O(1)-B(1)-O(2)	104.8(3)	N(4)-C(16)-C(17)	131.1(4)
C(2)-P(1)	1.854(4)	O(7)-B(1)-O(2)	113.5(3)	N(3)-C(16)-C(17)	122.8(4)
C(3)-C(4)	1.486(6)	O(8)-B(1)-O(2)	106.3(3)	C(18)-C(17)-C(16)	116.6(4)
C(4)-C(5)	1.368(6)	O(3)-C(1)-O(2)	124.4(4)	C(17)-C(18)-C(19)	120.8(4)
C(4)-N(1)	1.396(5)	O(3)-C(1)-C(2)	127.5(4)	C(20)-C(19)-C(18)	121.6(4)
C(5)-N(2)	1.382(5)	O(2)-C(1)-C(2)	108.1(3)	C(19)-C(20)-N(3)	117.9(4)
C(6)-N(2)	1.331(5)	O(1)-C(2)-C(1)	106.0(3)	C(10)-N(1)-C(6)	120.5(4)
C(6)-N(1)	1.377(5)	O(1)-C(2)-C(3)	111.1(3)	C(10)-N(1)-C(4)	129.9(4)
C(6)-C(7)	1.387(6)	C(1)-C(2)-C(3)	109.6(3)	C(6)-N(1)-C(4)	109.6(3)
C(7)-C(8)	1.350(7)	O(1)-C(2)-P(1)	106.6(3)	C(6)-N(2)-C(5)	110.0(3)
C(8)-C(9)	1.421(7)	C(1)-C(2)-P(1)	109.0(3)	C(16)-N(3)-C(20)	120.3(4)
C(9)-C(10)	1.362(6)	C(3)-C(2)-P(1)	114.2(3)	C(16)-N(3)-C(14)	110.1(3)
C(10)-N(1)	1.368(5)	C(4)-C(3)-C(2)	110.4(3)	C(20)-N(3)-C(14)	129.6(4)
C(11)-O(9)	1.202(5)	C(5)-C(4)-N(1)	105.5(4)	C(16)-N(4)-C(15)	109.1(4)
C(11)-O(8)	1.332(5)	C(5)-C(4)-C(3)	131.1(4)	C(2)-O(1)-B(1)	110.5(3)
C(11)-C(12)	1.527(6)	N(1)-C(4)-C(3)	123.5(4)	C(1)-O(2)-B(1)	110.4(3)
C(12)-O(7)	1.417(5)	C(4)-C(5)-N(2)	108.2(4)	C(12)-O(7)-B(1)	110.4(3)
C(12)-C(13)	1.544(6)	N(2)-C(6)-N(1)	106.7(4)	C(11)-O(8)-B(1)	110.8(3)
C(12)-P(2)	1.844(4)	N(2)-C(6)-C(7)	132.6(4)	O(5)-P(1)-O(4)	119.4(2)
C(13)-C(14)	1.483(6)	N(1)-C(6)-C(7)	120.7(4)	O(5)-P(1)-O(6)	109.81(17)
C(14)-C(15)	1.350(6)	C(8)-C(7)-C(6)	118.7(4)	O(4)-P(1)-O(6)	106.8(2)
C(14)-N(3)	1.405(5)	C(7)-C(8)-C(9)	121.0(4)	O(5)-P(1)-C(2)	110.48(19)
C(15)-N(4)	1.368(6)	C(10)-C(9)-C(8)	119.1(4)	O(4)-P(1)-C(2)	105.0(2)
C(16)-N(4)	1.353(5)	C(9)-C(10)-N(1)	120.0(4)	O(6)-P(1)-C(2)	104.28(18)
C(16)-N(3)	1.370(5)	O(9)-C(11)-O(8)	124.7(4)	O(11)-P(2)-O(12)	114.79(17)
C(16)-C(17)	1.388(6)	O(9)-C(11)-C(12)	126.6(4)	O(11)-P(2)-O(10)	107.5(2)
C(17)-C(18)	1.363(7)	O(8)-C(11)-C(12)	108.7(3)	O(12)-P(2)-O(10)	112.40(19)
C(18)-C(19)	1.405(7)	O(7)-C(12)-C(11)	105.4(3)	O(11)-P(2)-C(12)	109.71(18)
C(19)-C(20)	1.362(7)	O(7)-C(12)-C(13)	110.5(3)	O(12)-P(2)-C(12)	107.17(18)
C(20)-N(3)	1.375(5)	C(11)-C(12)-C(13)	110.3(3)	O(10)-P(2)-C(12)	104.81(18)
O(4)-P(1)	1.526(4)	O(7)-C(12)-P(2)	108.4(3)		

Table S4. Anisotropic displacement parameters ($\text{\AA}^2 \times 10^3$) for $\text{C}_{20}\text{H}_{14}\text{BN}_4\text{O}_{16}\text{P}_2$.

The anisotropic displacement factor exponent takes the form: $-2\pi^2[h^2 a^{*2}U^{11} + \dots + 2 h k a^* b^* U^{12}]$

	U ¹¹	U ²²	U ³³	U ²³	U ¹³	U ¹²
B(1)	15(2)	19(3)	21(3)	-2(2)	-3(2)	-4(2)
C(1)	23(2)	21(2)	29(3)	-6(2)	-2(2)	-1(2)
C(2)	22(2)	28(3)	38(3)	-14(2)	1(2)	-4(2)
C(3)	18(2)	36(3)	46(3)	-23(3)	1(2)	-4(2)
C(4)	29(3)	32(3)	42(3)	-17(2)	-15(2)	10(2)
C(5)	27(2)	22(2)	36(3)	-14(2)	-9(2)	0(2)
C(6)	17(2)	20(2)	27(3)	-8(2)	-4(2)	-1(2)
C(7)	18(2)	26(2)	22(2)	-5(2)	-3(2)	2(2)
C(8)	21(2)	20(2)	28(3)	-4(2)	-6(2)	-4(2)
C(9)	20(2)	18(2)	21(2)	-2(2)	-3(2)	-4(2)
C(10)	21(2)	23(2)	19(2)	0(2)	-4(2)	-3(2)
C(11)	28(2)	22(2)	24(3)	-6(2)	-5(2)	5(2)
C(12)	26(2)	36(3)	29(3)	-15(2)	-6(2)	2(2)
C(13)	22(2)	33(3)	43(3)	-12(2)	-2(2)	-5(2)
C(14)	28(3)	32(3)	32(3)	0(2)	2(2)	-3(2)
C(15)	27(2)	32(3)	19(2)	0(2)	-3(2)	-1(2)
C(16)	18(2)	19(2)	29(3)	-6(2)	-5(2)	3(2)
C(17)	26(2)	24(2)	27(3)	-4(2)	-5(2)	1(2)
C(18)	25(2)	25(3)	28(3)	-9(2)	-6(2)	-2(2)
C(19)	18(2)	20(2)	23(2)	-6(2)	-5(2)	-1(2)
C(20)	24(2)	21(2)	26(3)	-1(2)	-8(2)	-2(2)
N(1)	21(2)	19(2)	24(2)	-5(2)	-3(2)	-1(2)
N(2)	23(2)	25(2)	30(2)	-8(2)	-4(2)	-1(2)
N(3)	20(2)	19(2)	25(2)	-5(2)	-5(2)	2(2)
N(4)	24(2)	24(2)	27(2)	1(2)	-3(2)	3(2)
O(1)	30(2)	27(2)	27(2)	3(2)	-6(2)	-10(2)
O(2)	54(2)	23(2)	29(2)	1(2)	-19(2)	-6(2)
O(3)	52(2)	25(2)	56(3)	-8(2)	20(2)	-8(2)
O(4)	25(2)	27(2)	31(2)	-5(2)	-12(2)	-4(1)
O(5)	20(2)	19(2)	26(2)	-3(1)	-9(1)	-1(1)
O(6)	22(2)	17(2)	24(2)	-4(1)	-9(1)	0(1)
O(7)	19(2)	19(2)	22(2)	-5(1)	-3(1)	-3(1)
O(8)	20(2)	24(2)	19(2)	-3(1)	0(1)	-2(1)
O(9)	38(2)	30(2)	29(2)	-3(2)	-2(2)	-19(2)
O(10)	21(2)	26(2)	33(2)	-5(2)	-8(1)	4(1)
O(11)	28(2)	28(2)	23(2)	-7(1)	-1(1)	-4(1)
O(12)	25(2)	25(2)	29(2)	-4(1)	-9(1)	-5(1)
O(20)	45(2)	45(2)	39(2)	-2(2)	-7(2)	3(2)
O(21)	36(2)	31(2)	30(2)	4(2)	-11(2)	-12(2)
O(22)	57(3)	47(3)	47(3)	0(2)	-12(2)	2(2)
O(23)	70(3)	34(3)	179(7)	-35(3)	67(4)	-14(3)
P(1)	28(1)	20(1)	26(1)	1(1)	0(1)	-4(1)
P(2)	20(1)	19(1)	23(1)	-4(1)	-5(1)	-2(1)

Table S5. Hydrogen coordinates ($\times 10^4$) and isotropic displacement parameters ($\text{\AA}^2 \times 10^3$) for $\text{C}_{20}\text{H}_{14}\text{BN}_4\text{O}_{16}\text{P}_2$.

	x	y	z	U(eq)
H(3A)	8960	10524	4179	28
H(3B)	7814	10896	3372	28
H(5)	8365	8662	6267	28
H(7)	4213	6980	6318	36
H(8)	3139	7665	4681	43
H(9)	4003	9254	2975	40
H(10)	6010	10027	2919	33
H(13A)	8777	4168	2055	31
H(13B)	9790	5029	1035	31
H(15)	9507	3462	4273	32
H(17)	13539	5351	4173	35
H(18)	14395	6857	2449	41
H(19)	13318	7460	777	42
H(20)	11395	6574	783	35
H(21)	11350(40)	9740(40)	1410(40)	0(12)
H(22)	8370(60)	7070(60)	-700(60)	50(20)
H(23)	5120(50)	5670(50)	8460(50)	31(14)
H(24)	6010(100)	5580(90)	9390(100)	160(40)
H(2)	6471	7372	7089	32
H(4)	11411	3834	5024	33

Parameters and numerical results for Spartan calculations of dimer complexes of boron.

Output for RR

Number of shells: 161

Number of basis functions: 411

Multiplicity: 1

SCF model:

A restricted Hartree-Fock SCF calculation will be performed using Pulay DIIS + Geometric Direct Minimization

Optimization:

Step Energy Max Grad. Max Dist.

1	-2577.679174	0.081476	0.085455
2	-2577.731871	0.048966	0.074890
3	-2577.760928	0.030531	0.076737
4	-2577.770978	0.019101	0.062813
5	-2577.773615	0.009770	0.074885
6	-2577.774774	0.008286	0.056011
7	-2577.775583	0.010284	0.085350
8	-2577.776547	0.007853	0.108199
9	-2577.777370	0.012197	0.096527
10	-2577.778338	0.009290	0.134898
11	-2577.779188	0.009124	0.101273
12	-2577.779692	0.007069	0.104763
13	-2577.779515	0.012483	0.046241
14	-2577.780520	0.006508	0.066723
15	-2577.780779	0.004873	0.077441
16	-2577.781055	0.004102	0.063665
17	-2577.781335	0.004030	0.032589
18	-2577.781525	0.003658	0.057214
19	-2577.781733	0.003674	0.065537
20	-2577.781958	0.004189	0.071551
21	-2577.782250	0.003232	0.073724
22	-2577.782550	0.002992	0.070068
23	-2577.782841	0.004060	0.037014
24	-2577.783044	0.003526	0.042215
25	-2577.783179	0.003278	0.030072
26	-2577.783218	0.003131	0.028644
27	-2577.783248	0.002784	0.023885
28	-2577.783273	0.002255	0.024593
29	-2577.783285	0.002204	0.026632
30	-2577.783307	0.002759	0.026893
31	-2577.783328	0.002187	0.011101
32	-2577.783347	0.002359	0.014608
33	-2577.783366	0.002115	0.017854
34	-2577.783383	0.002324	0.023229
35	-2577.783413	0.002582	0.026607
36	-2577.783440	0.002380	0.020890
37	-2577.783459	0.002427	0.015486
38	-2577.783478	0.002020	0.009304
39	-2577.783495	0.001946	0.008863
40	-2577.783513	0.001661	0.010723
41	-2577.783529	0.001378	0.006323
42	-2577.783538	0.000998	0.003901
43	-2577.783543	0.000591	0.002967
44	-2577.783547	0.000367	0.002559
45	-2577.783550	0.000172	0.003852
46	-2577.783551	0.000121	0.001153

Reason for exit: Successful completion

Quantum Calculation CPU Time : 1:37:39.98
Quantum Calculation Wall Time: 1:40:27.83
SPARTAN '08 Properties Program: (PC/×86) Release 132
Reason for exit: Successful completion
Properties CPU Time : 4.05
Properties Wall Time: 4.19

Output for RS

Number of shells: 161
Number of basis functions: 411
Multiplicity: 1
SCF model:

A restricted Hartree-Fock SCF calculation will be
performed using Pulay DIIS + Geometric Direct Minimization
Optimization:

Step	Energy	Max Grad.	Max Dist.
1	-2577.676182	0.066036	0.090712
2	-2577.729882	0.045007	0.073872
3	-2577.759333	0.025576	0.088634
4	-2577.769484	0.012252	0.091373
5	-2577.773479	0.006663	0.084285
6	-2577.776184	0.007370	0.083197
7	-2577.778151	0.009319	0.073293
8	-2577.779663	0.014708	0.071188
9	-2577.780716	0.011412	0.081350
10	-2577.781457	0.016341	0.094951
11	-2577.782079	0.010137	0.041264
12	-2577.782775	0.010029	0.041196
13	-2577.783385	0.010230	0.053626
14	-2577.783632	0.006671	0.032460
15	-2577.783860	0.009689	0.034482
16	-2577.784041	0.008405	0.050175
17	-2577.784204	0.008235	0.052582
18	-2577.784403	0.007018	0.095961
19	-2577.784637	0.005946	0.100752
20	-2577.784867	0.005338	0.106192
21	-2577.785146	0.005536	0.127900
22	-2577.785464	0.004265	0.101086
23	-2577.785843	0.007310	0.103763
24	-2577.786269	0.008199	0.108093
25	-2577.786741	0.011026	0.102298
26	-2577.787078	0.012211	0.096353
27	-2577.787363	0.012625	0.087728
28	-2577.787583	0.011683	0.065790
29	-2577.787787	0.008680	0.060423
30	-2577.788089	0.008186	0.072112
31	-2577.788340	0.007020	0.022992
32	-2577.788564	0.006163	0.057685
33	-2577.788921	0.003815	0.049761
34	-2577.789112	0.004144	0.058509
35	-2577.789345	0.005438	0.051949
36	-2577.789543	0.003767	0.048768
37	-2577.789683	0.002666	0.014632
38	-2577.789773	0.002638	0.012514
39	-2577.789827	0.002977	0.014069
40	-2577.789859	0.002664	0.008578
41	-2577.789885	0.002426	0.008944

42 -2577.789912 0.001811 0.012225
43 -2577.789937 0.001444 0.011812
44 -2577.789962 0.001193 0.014188
45 -2577.789981 0.000872 0.012184
46 -2577.789994 0.000729 0.015445
47 -2577.790004 0.000404 0.011521
48 -2577.790010 0.000319 0.007656
49 -2577.790012 0.000200 0.003859
50 -2577.790013 0.000163 0.001841
Reason for exit: Successful completion
Quantum Calculation CPU Time : 1:43:12.91
Quantum Calculation Wall Time: 1:45:10.06
SPARTAN '08 Properties Program: (PC/x86) Release 132
Reason for exit: Successful completion
Properties CPU Time : 4.05
Properties Wall Time: 4.08

Reference List

1. C. E. McKenna, B. A. Kashemirov, K. M. Błażewska, I. Mallard-Favier, C. A. Stewart, J. Rojas, M. W. Lundy, F. H. Ebetino, R. A. Baron, M. L. Kirsten, J. E. Dunford, M. C. Seabra, J. L. Bala, M. S. Marma, M. J. Rogers and F. P. Coxon, *J. Med. Chem.*, 2010, **53**, 3454-3464.
2. SMART V 5.63, Software for the CCD Detector System, Bruker AXS Madison, WI, 2002.
3. SAINT PLUS V 6.54 A, Software for the CCD Detector System. Bruker AXS Madison, WI, 2003.
4. SADABS, Software for the CCD Detector System, Bruker AXS Madison, WI, 2003.
5. G. M. Sheldrick, SHELXS-90, Program for the Solution of Crystal Structure, University of Göttingen, Germany, 1990, SHELXL-97, Program for the Refinement of Crystal Structure, University of Göttingen, Germany, 1997; SHELXTL 6.14 for Windows NT/2000, Program library for Structure Solution and Molecular Graphics, Bruker AXS, Madison, WI, 2003.
6. L. J. Farrugia, *J. Appl. Cryst.*, 1997, **30**, 565.